A New Streamline Curvature Throughflow Method for Radial Turbomachinery

Michael Casey
ITSM-Institute of Thermal Turbomachinery and Machinery Laboratory,
Universität Stuttgart,
Pfaffenwaldring 6,
D-70569 Stuttgart, Germany
e-mail: michael.casey@itsm.uni-stuttgart.de

Chris Robinson
PCA Engineers Limited,
Studio 2, Deepdale Enterprise Park,
Deepdale Lane,
Nettleham,
Lincoln LN2 2LL, UK
e-mail: chris.robinson@pcaeng.co.uk

This paper describes a newly developed streamline curvature throughflow method for the analysis of radial or mixed flow machines. The code includes curved walls, curved leading and trailing edges, and internal blade row calculating stations. A general method of specifying the empirical data provides separate treatment of blockage, losses, and deviation. Incompressible and compressible fluids are allowed, including real gases and supersonic relative flow in blade rows. The paper describes some new aspects of the code. In particular, a relatively simple numerical model for spanwise mixing is derived; the calculation method for prescribed pressure ratio in compressor blade rows is described; and the method used to redistribute the flow across the span due to choking is given. Examples are given of the use and validation of the code for many types of radial turbomachinery, and these show that it is an excellent tool for preliminary design.
[DOI: 10.1115/1.3151601]

1 Introduction

In most turbomachinery design systems a meridional throughflow calculation is the backbone of the design process. It is fast, reliable, easy to understand, deals easily with multiple blade rows, and includes empirical loss, deviation, and blockage correlations. Performance and experience from earlier machines can then be taken into account in the preliminary design, in a way which is not easy with 3D computational fluid dynamics (CFD).

Most throughflow codes use the streamline curvature method and derive from those of Smith [1], Novak [2], and Denton [3], based on the general S1/S2 theory of Wu [4]. Other methods of solving the equations have been looked at [5–8], but none have displaced streamline curvature in practice, as in throughflow methods the "accuracy is determined by the accuracy of the correlations rather than the numerics" (quotation from Ref. [3]).

This paper describes a streamline curvature meridional throughflow method for radial turbomachinery known as VISTA TF. It is a completely new coding of streamline curvature throughflow theory based on the method of Denton [3] and its adaptation to radial compressors by Casey and Roth [9], but with many new features. The streamline curvature approach is used to solve the throughflow equations, rather than a more modern numerical technique, as the theory is easy to understand, being based on the spanwise equilibrium of a circumferentially-averaged flow in an annulus. It automatically leads to clearly defined meridional streamlines, which neatly allow a blade-to-blade and throughflow view of the turbomachine for design purposes. In addition it can be used in a "ductflow" mode, with only leading and trailing edges of the blade rows defined, which often is an advantage in the preliminary design phase of multistage axial machines.

There are two main disadvantages of the streamline curvature technique. First, it allows no reverse flow in the meridional plane. Nowadays, however, issues of flow separation are best resolved with a fully viscous 3D CFD solution rather than with a 2D throughflow method. It is more important that a throughflow code identifies the problem without breaking down, so that appropriate design decisions can be made to try to avoid the reverse flow. Second, the method suffers from a sharp increase in calculating time on grids with finely spaced quasi-orthogonal lines owing to the stability requirements of the streamline curvature calculation [10]. However, the calculating time of a throughflow code on a modern laptop for a radial stage is only a few seconds, so this is also relatively unimportant.

The code described here is primarily designed for single stage radial turbomachinery applications, but there is no limitation in the code, which forbids its use for any multistage axial or radial turbomachinery application. Key features of the code are listed below.

- Highly curved annulus walls are allowed, providing a simple definition of axial and radial wall geometries and any combination of these.
- Any combination of blade row calculating stations, together with duct flow regions, can be used in the domain allowing all types of turbomachinery to be calculated.
- Curved quasi-orthogonal lines allow blades with sweep and curved leading and trailing edges to be modeled.
- Internal blade row calculating stations are used, not just leading and trailing edges, and blade force terms are included to take into account the lean of the blades, whereby the body force is assumed to act normal to the blade camber surface.
- A general method of taking into account the spanwise variation in empirical data for losses, deviation, and blockage has been programmed, including spanwise distributed blockage in the continuity equation and the use of entropy loss coefficients and dissipation coefficients.
- Dissipation force terms are used in the radial equilibrium equation, although this is mainly of academic interest.
- Compressible and incompressible fluids are possible, including supersonic relative flow in blade rows.
- Blade row choking is not just included as additional loss, but its effect on the redistribution of the meridional flow distribution is taken into account.
- In blade rows with sufficient number of internal planes, an approximation for the blade-to-blade flow field is calculated, which includes the effect of splitter vanes.
- Spanwise mixing of angular momentum, total enthalpy, and entropy across the meridional streamtubes are taken into account by a new model, which accounts for turbulent diffusion and deterministic secondary flows.

Contributed by the International Gas Turbine Institute of ASME for publication in the JOURNAL OF TURBOMACHINERY. Manuscript received August 19, 2008; final manuscript received February 4, 2009; published online April 7, 2010. Review conducted by David Wisler. Paper presented at the ASME Turbo Expo 2008: Land, Sea and Air (GT2008), Berlin, Germany, June 9–13, 2008.

- The code can operate with specified mass flow, pressure ratio, or specified outlet swirl.
- A restart from a previously converged solution reduces the effort for a new calculation with changed geometry or modified flow parameters and boundary conditions, which is useful in combination with optimization methods.

Some of these features have either been described in earlier papers on streamline curvature methods, or are relatively straightforward extensions of earlier throughflow methods, and so are not described in detail here. This paper provides a general introduction to the method used and then concentrates on the completely new aspects of the models in the code and their implementation. The new features include the way in which losses are taken into account, the use of the code as a mean-line tool, a built-in simplified blade-to-blade model with blending functions for the swirl generation, a new model for spanwise mixing, iteration to pressure ratio for choked compressor blade rows, redistribution of flow due to choked streamlines, and inclusion of different fluids. In addition to describing these new features some details of the validation and verification of the code are given.

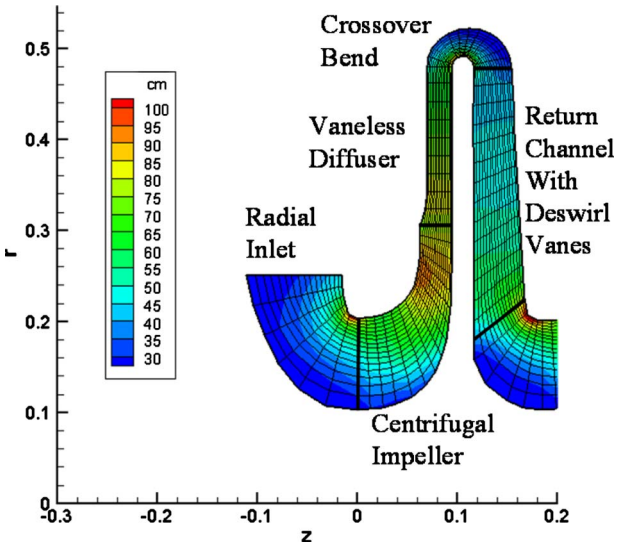

Fig. 1 Industrial radial compressor stage showing streamlines and calculating stations and the meridional velocity distribution

2 Streamline Curvature Throughflow

Many publications derive the equations for the streamline curvature throughflow method, so only an overview is given here. The reader who needs more detail should consult two recent books, which give a thorough discussion of the method, Refs. [11,12], or refer to the original papers already quoted.

The equations solved are the continuity equation, the energy equation (a combination of the first law of thermodynamics and the Euler equation of turbomachinery), a suitable equation of state and the inviscid momentum equation for the flow on the mean stream surface (in the form of the general radial equilibrium equation). The mean stream surface has roughly the form of the blade camber surface and requires geometrical input and empirical information (incidence and deviation) to determine its precise shape.

The grid for the calculation is based on fixed calculating stations, which are roughly normal to channel walls, and the streamlines of the mean circumferentially-averaged flow in the meridional direction. The meridional streamline grid is not fixed, apart from the hub and shroud streamlines on the annulus walls, but changes continually during the iterations. The fixed calculating stations are oriented with the leading and trailing edges, so need to be curved if these are curved and can be in duct regions, which is in the blade-free space upstream and downstream of blades, at the leading and trailing edges of the blades and internally within the blades. By suitable combinations of different types of calculating stations, any type of turbomachine can be modeled. An example of the grid for a single stage compressor with radial inlet, centrifugal impeller, vaneless diffuser, crossover bend, and return channel with deswirl vanes is shown in Fig. 1. This is the first stage of a 9 stage multistage radial compressor with 17 blade rows that has been simulated with this method. The grid density shown in Fig. 1 is typical of that used, with 15 planes for a radial impeller.

The solution method is iterative in terms of several variables (primarily the meridional velocity, but also the density, streamline location, etc.), all of which progressively converge from an initial estimate to a final solution within nested iterations. The momentum equation on the mean stream surface is a generalized form of the radial equilibrium equation, developed to give an expression for the spanwise gradient of the meridional velocity along a calculating station

$$c_m \frac{dc_m}{dq} = \frac{dh_t}{dq} - T\frac{ds}{dq} - \frac{1}{2r^2}\frac{d(r^2c_u^2)}{dq} + \sin\psi\frac{c_m^2}{r_c} + \cos\psi c_m\frac{\partial c_m}{\partial m} + \tan\gamma\frac{c_m}{r}\frac{\partial(rc_u)}{\partial m} + F_d \quad (1)$$

The gradient of the meridional velocity is related to the curvature and the current positions of the streamlines, to the orientation of the mean stream surface (angles ψ and γ), and to the flow parameters from the previous iteration. There are several forms of this velocity gradient equation. Equation (1) follows the method of Denton [3], but takes into account the blade force terms, as described by Cumpsty [11], and the dissipation force terms, as given by Horlock [13], essentially as previously described by Casey and Roth [9].

The velocity gradient equation is solved in combination with a method for finding the correct velocity level on the mean streamline that ensures that the flow across the calculating station satisfies the continuity equation

$$\dot{m} = \int k\rho c_m \sin\psi dq \quad (2)$$

where k is an empirical blockage factor, and ψ is the angle between the streamline direction and the calculating station. The meridional velocity on the mean streamline at each calculating station is specified in the innermost iteration, integrated across the flow channel with the help of the velocity gradient, Eq. (1), and then continually updated until the mass flow is correct. Care is needed in this process with transonic flows, as at $M=1$ there is no variation in the mass flow with a change in meridional velocity.

The meridional velocity distribution determines the position of the streamlines of the flow on all calculating stations. These positions are continually updated for each calculating station in an outer iteration as the program converges. The streamline positions are used to interpolate new blade element data appropriate to their current location and to find the slopes and curvatures of the streamlines and derivatives of the flow parameters along the streamlines, which are needed in the velocity gradient equation, Eq. (1).

Between blade rows, the total enthalpy and angular momentum are convected along the meridional streamlines from the previous station. The entropy would also be convected in an inviscid flow, but the additional viscous losses cause it to increase in the direc-

tion of the flow. In blade rows the changes in momentum and enthalpy are calculated from the Euler equation on the assumption that the flow follows the mean stream surface. The mean stream surface is only roughly aligned with the camber surface of the blade. It points in the true flow direction taking into account the incidence and deviation of the flow, using empirical correlations.

The equation of state is best solved in the form of a Mollier diagram, such as $p=f(h,s)$, as the enthalpy is derived from the Euler equation and the entropy from the losses. For liquids and ideal gases analytical equations are used but for real gases interpolation in tables is needed.

At the inlet plane the variation of total pressure, total temperature and angular momentum or flow angle together with the gas data are defined. At the outlet plane the mass flow is usually given, but for calculations with choked flows it is necessary to specify the outlet static pressure, such that the mass flow is a result of the simulation.

3 Empirical Information

Empirical methods are used to provide data for the loss production, for the boundary layer blockage and for the deviation of the flow direction from the mean blade camber surface, so that the effect of viscous losses can be taken into account. The three main effects of the empirical data are as follows.

- In the equation of state, a change in the entropy through dissipation losses leads to a pressure loss for a given value of the total enthalpy.
- In the continuity equation, the blockage due to the endwall boundary layer displacement thickness leads to a higher value of the meridional velocity.
- In the momentum equation, the deviation of the flow from the blade camber direction changes the mean stream surface and the swirl velocity.

There are numerous possible combinations of data for the empirical information, based on various definitions of loss coefficients, dissipation coefficients, and efficiencies and so on, and this leads to the largest source of confusion in the data preparation for any throughflow code, and many internal branches within typical codes. In this new code the treatment of the blockage, loss, and the deviation is separated so that individual correlations for each effect can be applied. Where possible the correlations for 2D effects (such as profile losses) and for 3D effects (endwall and clearance effects) are also separated. Spanwise variations of each of these can be specified by the user or determined from built-in correlations.

Some aspects of the deviation model will be described in Sec. 4. Many throughflow methods work with a fixed value of the blockage for all streamlines, such that in the flow is considered to be in a "blocked" channel. In the present method, the blockage model includes spanwise distributed blockage, i.e., the value of the blockage factor k in Eq. (2) can vary across the span.

In the solution of the throughflow equations, a single form of loss definition based on the entropy rise, following Ref. [14] is used, as follows:

$$\chi_{\text{turbine}} = T_1(s_2 - s_1)/\left(\tfrac{1}{2}c_2^2\right)$$

$$\chi_{\text{compressor}} = T_1(s_2 - s_1)/\left(\tfrac{1}{2}c_1^2\right)$$

This entropy-based loss coefficient is shown by Denton [14] to be numerically the same as a kinetic energy loss coefficient. It directly determines the change in entropy, which can be immediately used in the equation of state and in Eq. (1). In this way it is not only easier to code, but it is also probably a more precise way of including losses in the calculation. Other more common forms of loss coefficient, such as the pressure loss coefficients determined by the many correlations included in the code, first have to be converted internally to an entropy loss coefficient, using the equations given by Brown [15], before they can be used by the code.

In addition to loss coefficients or polytropic efficiency, the code can calculate the losses from dissipation coefficients, which also directly predict the entropy increase. A single value of the dissipation coefficient for a calculating station is specified, and this value is then used to estimate the total rate of entropy production on the wetted surfaces due to the boundary layer dissipation based on the integration of

$$T\dot{S}_{\text{total}} = \rho c_d \int w^3 dA$$

where w is the local surface relative velocity at the edge of the boundary layer. In a duct region the integration is carried out on the hub and casing walls, and in a blade row the integration includes the dissipation on the suction and pressure surfaces using the local relative surface velocities. The total entropy production is then used to determine a mean specific entropy increase from one calculating station to the next, and this is applied on each streamline.

As the code allows for liquids, ideal gases, and real gases, some care is needed in the determination of efficiency from the results, and aspects of the calculation of efficiency in the code have already been published in Ref. [16].

4 Blade-to-Blade Solution

The solution on the mean stream surface provides the flow field in the meridional plane through the turbomachine, and this needs to be combined with a blade-to-blade method to find blade surface velocities. In traditional S1/S2 methods this is done with the help of an additional S1 blade-to-blade method. The current code includes blade internal calculating stations and, if sufficient of these are present to calculate a reasonable estimate of the streamwise gradient of swirl, then this can be used to estimate the blade-to-blade loading from the local circumferential blade force, similar to Ref. [17], as follows:

$$-\frac{\partial p}{\partial \theta} = (\rho c_m)\frac{\partial (rc_u)}{\partial m}$$

The method computes the flow based on the geometry of the mean stream surface. This is not congruent with the mean camber surface, and the differences (due to incidence and deviation) have to be taken into account by empirical modifications. This is done with blending functions, which adapt the swirl generation in the blade row to allow the camber surface to be partly transparent to the flow, such that the flow angle differs from the blade angle as outlined by Traupel [18] and used by Casey and Roth [9]. A similar approach using so-called "departure angles" is described by Smith [19].

When calculating radial turbomachinery of high solidity, the blending functions on the swirl are used in the inlet region, and the departure angle approach is used in the trailing edge region. Extensive tests on many different types of blade row have demonstrated that this is the most effective approach in high solidity blade rows and leads to sensible estimates for the blade-to-blade loading in the inlet and outlet regions of the blade. The angular momentum of the flow relative to the blade row is calculated as follows:

$$(rw_u)_{i,j} = (\gamma_{\text{in}})_{i,j}(rw_u)_{\text{in}} + [(rc_m)_{i,j}\tan(\beta'_{i,j} + \delta_{te}(\gamma_{\text{out}})_{i,j})][1 - (\gamma_{\text{in}})_{i,j}]$$

The actual values of the swirl at inlet and the deviation angle at outlet (determined by the deviation or slip correlations) need to be updated in each iteration. The blending functions (γ_{in} and γ_{out}) follow the approach of Wilkinson [20].

Figure 2 shows the predicted suction surface and pressure surface static pressure distribution along the mean meridional streamline of a radial impeller, calculated using 3D CFD (ANSYS CFX11) and the approximate blade-to-blade method. Although the simpli-

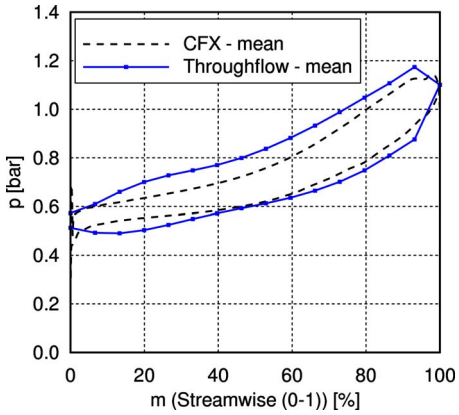

Fig. 2 Suction and pressure surface static pressure distribution along the mean meridional streamline of a radial impeller calculated with 3D CFD (CFX) and with throughflow

fied method is not perfect, it is clearly sufficiently accurate to guide the designer to make sensible design decisions about blade loading distributions.

5 Spanwise Mixing

A major shortcoming of the basic streamline curvature method is the neglect of spanwise transport of angular momentum, energy, and losses in the direction normal to the streamlines. By definition, a throughflow code is based on the assumption that the flow remains in concentric streamtubes as it passes through the turbomachine, and no mass transfer occurs across the meridional streamlines, which are the streamtube boundaries. So for example, in a duct region of a throughflow calculation enthalpy, angular momentum (swirl) and entropy are conserved along the streamlines.

In reality, there are several mechanisms that lead to an apparent spanwise transport of fluid relative to flow on the mean streamlines, as follows:

- twisted blade-to-blade stream surfaces as result of streamwise vorticity being shed by the blades (stream surface twist)
- secondary flows in the endwall boundary layers and in the blade boundary layers
- wake momentum transport downstream of blade rows
- tip clearance flows with tip clearance vortices
- turbulent diffusion

If realistic loss levels are specified for the end-wall regions, and spanwise mixing is neglected, then unrealistic profiles of the loss occur after several blade rows, as there is no mechanism for the high losses generated near the end-walls to be mixed out. The simplest approach to deal with this problem is to specify unrealistic loss distributions across the span, in order to avoid high levels in the end-walls. In fact, in preliminary design calculations it is often adequate to specify a mean-line value of loss and to assume that the entropy generated is the same on each streamtube. This approximates a complete mixing of the losses across the span.

More sophisticated methods to include the physics of these mixing processes have been attempted so that realistic loss distributions can be specified. The common approach is to model the spanwise mixing as a turbulent diffusion, even though some of the effects are due to deterministic flow features. Spanwise mixing is needed to mix out the high losses close to the endwalls, but the precise model of how the mixing is included appears not to be particularly important [21–24].

The model in this code follows that described by Denton and Hirsch [21]. Improvements to this are guided by the turbulent

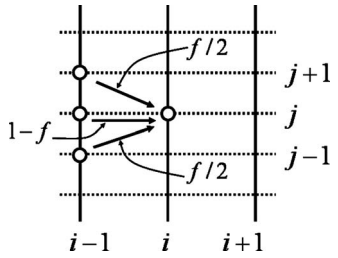

Fig. 3 Mixing factor model proposed by Denton and Hirsch [21]

diffusion model of Lewis [24]. The model assumes that some proportion of the local flow is spread across the streamlines by deterministic spanwise flows. In a duct flow, the entropy, angular momentum (swirl), and total enthalpy on a particular grid point are determined mainly by the values on the same streamline at the upstream station and partly by the values transferred from the adjacent streamlines. A fraction of the flow $(1-f)$ is convected along the streamlines and a fraction $\left(\frac{1}{2}f\right)$ is transferred from each of the two adjacent streamlines, where f is a mixing factor with a value less than unity, see Fig. 3.

The value of the convected parameter P is first calculated on the assumption of no mixing and this is then modified by a small amount due to mixing as follows:

$$\Delta P_{i,j} = (-f)P_{i-1,j} + (f/2)P_{i-1,j+1} + (f/2)P_{i-1,j-1}$$

In this way a fraction f of the conserved parameter P diffuses away from the streamline (actually $f/2$ to the upper streamline and $f/2$ to the lower streamline), and a fraction $f/2$ of the values on the upper and the lower streamlines diffuses to this streamline. This can also be written in the following form:

$$\Delta P_{i,j} = (f/2)[(P_{i-1,j+1} - P_{i-1,j}) - (P_{i-1,j} - P_{i-1,j-1})]$$

If we write the difference between the parameter P on adjacent streamlines as

$$\delta P_{i-1,j+1} = P_{i-1,j+1} - P_{i-1,j} \quad \text{and} \quad \delta P_{i-1,j} = P_{i-1,j} - P_{i-1,j-1}$$

we obtain

$$\Delta P_{i,j} = (f/2)(\delta P_{i-1,j+1} - \delta P_{i-1,j}) \tag{3}$$

Note that with a positive gradient in P along the calculating station, there is a positive contribution to the value from the upper streamline and a negative contribution from the lower streamline due to mixing, and if the gradient is constant then this leads to no change in the parameter P.

This model is very effective in causing mixing as the flow proceeds downstream, but it has a large drawback as a general model: If the meridional grid spacing, or the number of streamlines, is changed, then a different value of the mixing factor is needed to produce the same level of spanwise mixing. Denton suggested simply that a value of $f=0.5$ should be used to cure any problems of entropy buildup in multiblade-row calculations. This disadvantage can be overcome if a turbulent diffusion equation is used to determine the strength of the mixing factor, as explained below.

Following the approach of Lewis, we assume that the spanwise mixing of a parameter P, which may be angular momentum, total enthalpy, or entropy, is determined by a diffusion equation of the type

$$c_m \frac{\partial P}{\partial m} = \varepsilon \frac{\partial^2 P}{\partial q^2}$$

where m is the meridional direction, q is the spanwise direction, P is the parameter undergoing spanwise mixing, and ε is a diffusion coefficient. For simplicity in this model q is taken as the distance along the quasi-orthogonal rather than the exact spanwise direc-

tion, although this simplification could easily be removed if necessary. For a small step along the meridional streamline we obtain that the change in the parameter P due to spanwise mixing by diffusion is given by

$$\Delta P = \frac{\delta m}{c_m} \varepsilon \frac{\partial^2 P}{\partial q^2}$$

The second derivative along the calculating station can be written as

$$\frac{\partial^2 P}{\partial q^2} = \frac{\partial}{\partial q}\left(\frac{\partial P}{\partial q}\right)$$

If the gradient of parameter P is constant, then this term is zero and no spanwise mixing takes place, as the spanwise transfer due to diffusion of P from the streamline with the higher value is compensated by the spanwise transfer from the adjacent streamline with the lower value.

An approximate value of this second derivative is

$$\frac{\partial^2 P}{\partial q_{i,j}^2} = \frac{2}{q_{i,j+1} - q_{i,j-i}}\left(\frac{P_{i-1,j+1} - P_{i-1,j}}{q_{i,j+1} - q_{i,j}} - \frac{P_{i-1,j} - P_{i-1,j-1}}{q_{i,j} - q_{i,j-1}}\right)$$

and, if the streamlines are evenly spaced, we obtain

$$q_{i,j+1} - q_{i,j-i} = 2(q_{i,j+1} - q_{i,j}) = 2(q_{i,j} - q_{i,j-1}) = 2\delta q_{i,j}$$

The second derivative of P can be approximated by

$$\frac{\partial^2 P}{\partial q_{i,j}^2} \approx \frac{1}{\delta q_{i,j}^2}[(P_{i-1,j+1} - P_{i-1,j}) - (P_{i-1,j} - P_{i-1,j-1})]$$

so that we obtain

$$\frac{\partial^2 P}{\partial q_{i,j}^2} = \frac{1}{\delta q_{i,j}^2}(\delta P_{i-1,j+1} - \delta P_{i-1,j})$$

The change in parameter P due to spanwise mixing becomes

$$\Delta P_{i,j} = \frac{\delta m_{i,j}}{c_{m,i,j}} \frac{\varepsilon_{i,j}}{\delta q_{i,j}^2}(\delta P_{i-1,j+1} - \delta P_{i-1,j})$$

This includes a positive contribution transferred from the upper and the lower streamtubes and a loss due to diffusion to these streamtubes. By comparison with Eq. (3), it can be seen that this is formally identical to the mixing factor algorithm. This algorithm is equivalent to the solution of the diffusion equation if the mixing factor is directly related to the physical diffusion coefficient as follows:

$$f/2 = \frac{\delta m_{i,j}}{c_{m,i,j}} \frac{\varepsilon_{i,j}}{\delta q_{i,j}^2} \tag{4}$$

The actual value of the mixing factor f is not a constant but needs to be changed throughout the flowfield. More diffusion, wider spacing of the quasi-orthogonals, lower spacing of the streamlines, or a lower value of the meridional velocity all require a higher value of the mixing factor.

Equation (4) can also be written as the product of two dimensionless terms

$$f/2 = \left(\frac{\varepsilon_{i,j}/c_{m,i,j}}{\delta q_{i,j}}\right) \Big/ \left(\frac{\delta q_{i,j}}{\delta m_{i,j}}\right)$$

The numerator represents the rate of spread of parameter P across the streamlines under the influence of diffusivity. The denominator is related to the grid structure, as it is the tangent of the angle between adjacent neighboring points and represents the spread of the grid. In this way it can be seen that the mixing factor needs to be adjusted to take into account the spread of parameter P relative to the spread of the grid.

This exposes a clear weakness of the method. If the grid has wide spacing along the meridional direction together with small spanwise distances between the streamlines, the factor f becomes very large. Clearly it is not sensible if this becomes too large. With a value of the mixing factor of 0.5, as suggested by Denton, the algorithm causes the flow on any particular streamline to have the same influence as that from the adjacent streamlines and more mixing than this is not really possible across a single streamtube.

A second weakness is that the algorithm as given above only accounts for changes that take place across a single streamtube. At high mixing levels or with closely spaced streamlines the next adjacent streamtubes are also affected by diffusion, so that some of the conserved parameter on these streamtubes is also transferred to the streamline under consideration. If we assume a constant grid spacing from streamline to streamline and examine the contribution to parameter P that is transferred by diffusion from all adjacent streamlines we obtain the result that this effect diminishes with the square of the grid spacing, as shown in Eq. (4) above. Taking into account the effect from all streamtubes gives additional terms in the mixing algorithm so that the positive contribution from all adjacent streamtubes is

$$\Delta P_{i,j}^{+} = \ldots + (f_{j+3}/18)P_{i-1,j+3} + (f_{j+2}/8)P_{i-1,j+2} + (f_{j+1}/2)P_{i-1,j+1} + (f_{j-1}/2)P_{i-1,j-1} + (f_{j-2}/8)P_{i-1,j-2)} + (f_{j-3}/18)P_{i-1,j-3}\cdots$$

The negative contribution that is lost from the local streamline is given by

$$\Delta P_{i,j}^{-} = (f_j + f_j/4 + f_j/9 + f_j/16 + \cdots)P_{i,j}$$

The maximum value of the infinite series here is such that if no more than 100% of the local value can be diffused away, this leads to a maximum value of the mixing factor of

$$f_j = 6/\pi^2 \approx 0.6$$

In the current mixing algorithm the first four terms in this series are taken into account, so a minimum of nine streamlines are needed if spanwise mixing is used.

The analysis above shows formally that, with the appropriate coefficients and adjustment to take into account the effect over several streamtubes, the mixing factor model can be identified with a turbulent diffusion equation and so can be used to model this effect by appropriate tuning of the mixing factor. The mixing factors associated with each individual source of spanwise transport in each streamtube (including turbulent diffusion) can be combined to obtain the cumulative effects. In practice, the code makes use of this algorithm, but uses a mixing factor determined from a user-specified eddy diffusion coefficient from Eq. (4). In the interest of simplicity, the actual value of the mixing factor is calculated separately for each streamline in the flowfield based on constant values of the diffusion coefficient, and the same value of f is used to redistribute the parameter P upward and downward to adjacent streamlines. This approach ensures that the spanwise mass-averaged values of the parameter P on the calculating station are conserved despite the mixing between the streamlines. In addition, the algorithm takes into account the nonuniform spacing of the streamlines and the special streamlines close to the wall, where only one adjacent streamline is present.

The data given by Gallimore [23] and Lewis [24] identify a physically realistic value for the diffusion coefficient ε, scaled with the mean meridional velocity and the stage length for axial turbines and compressors. There is considerable scatter between different machines and different operating points. A larger value is needed where spanwise mixing is high due to deterministic effects (secondary flows, streamsurface twist, etc.), and a lower value is required to account for pure turbulent mixing, which is higher in compressors than in turbines. In the current calculations the actual value for the mixing coefficient used is based on the numerical values of Gallimore and Lewis but is scaled by a reference velocity and the reference diameter of the calculation, as follows:

$$\varepsilon = 0.0001 \; u_{\text{ref}} D_{\text{ref}} \tag{5}$$

In radial turbomachinery the reference condition is impeller outlet for compressors and impeller inlet for turbines.

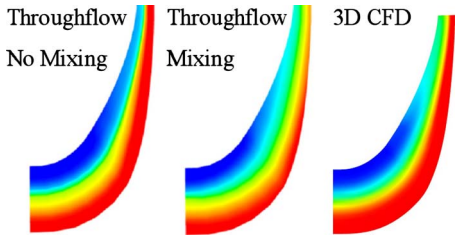

Fig. 4 The effect of spanwise mixing on the temperature stratification in a refrigeration impeller with a cold sidestream. Left: no mixing, middle: mixing (Eq. (5)), and right: 3D CFD.

The mixing algorithm has been incorporated to redistribute the pressure losses generated by the endwall boundary layers, but an example of its use for another purpose is shown in Fig. 4. This shows a simulation of a radial impeller for an ethylene refrigeration application with a cold sidestream. In the calculation with no mixing the cold (casing) and warm (hub) inlet flows do not mix through the whole compressor and remain stratified to the outlet. Using the spanwise mixing model with a diffusion coefficient given by Eq. (5), as recommended above, leads to mixing, which closely matches that of a CFD simulation of this impeller.

6 Choking

Before discussing how choked flows are calculated three important points need to be made. First it should be noted that the throughflow method is not particularly well suited for choked blade rows. The mean stream surface equations average out the flow in the circumferential direction and are thus not really aware of any high Mach numbers on the suction surface of blades. In addition, any shocks that may be present in turbomachinery flows are generally not oriented in the circumferential direction, so they are smeared out in the circumferential averaging of the flow to determine the mean stream surface. Nevertheless, despite these serious limitations an attempt has been made to model choking in the blade rows so that, in combination with correlations, the maximum flow and the additional losses related to shocks are taken into account in the overall predicted performance. In this way the code includes aspects of choking that are compatible with the level of empiricism of typical 1D calculation methods. This is useful in a code intended for design purposes, as it identifies choking problems early in the design process, and aids the understanding of the matching of the blade rows as the rotational speed varies.

Second, in a fully choked flow it is better to calculate with a specified pressure ratio rather than with a specified mass flow. Simulations in which the specified mass flow exceeds the choking mass flow lead to a physically impossible solution, and there are many solutions with different pressure ratios available for the choking mass flow. Denton [3] explained very briefly how to solve this problem for turbine blade rows, where choking takes place near the trailing edge based on the so-called "target pressure" method, which is also described in more detail by Came [25]. The new code includes these techniques for turbines, but this has now been extended to compressor applications where choking occurs near the leading edge.

Third, choking occurs at the throat between two blades. Although the throat is generally not a calculating plane of the throughflow calculation, it can be used as a virtual plane to assess whether the streamline concerned is choked and to limit the mass flow accordingly. A good estimate of the choking flow should make use of accurate estimates of the throat areas and throat position, so the throughflow code needs to be combined with a geometry definition system to ensure that the throats and throat positions are well-defined. This is not a practical limitation, as the blade geometry data and the channel geometry also have to be prepared by such a program.

The choking calculation can be considered to be a straightforward extension of the simple one-dimensional isentropic flow of a perfect gas through a stream-tube of varying area. Classical one-dimensional gas dynamics then determines the mass flow per unit streamtube area as a function of the Mach number and the maximum mass flow per unit area at a throat Mach number of unity. In a throughflow calculation we do not have a one-dimensional flow but have a series of individual streamtubes across the span. The choking of each individual streamtube must be analyzed on a one-dimensional basis, and the maximum possible mass flow for the calculating station can then be calculated by integrating the maximum mass flow at each streamtube across the span. In this process an individual streamtube on a particular station can be choked, but others are still able to pass more flow so the whole calculating plane is not yet choked.

Close to the leading edge of a compressor and near to the trailing edge of a turbine the maximum value of the local mass flow per unit streamtube width is limited by the throat to be

$$\dot{m}'_{\max,\mathrm{th}} = Zo\frac{p_t}{\sqrt{RT_t/\gamma}}\left(\frac{\gamma+1}{2}\right)^{-(\gamma+1)/(2(\gamma-1))}$$

The equation for the maximum flow across the calculating station adjacent to the throat is then determined by integration across the span as

$$\dot{m}_{\max,\mathrm{th}} = \int (k\dot{m}'_{\max,\mathrm{th}} \sin\psi)dq$$

At a turbine outlet, the procedure used is similar to that described by Denton [3] and Came [25], so this will be described first. They assumed that the choking of a turbine always occurs at the throat, which is taken to be close to the turbine trailing edge plane. Their calculations were generally for axial blade rows without internal planes, and they assumed that there are no relative total pressure losses along a streamtube between the turbine leading edge inlet plane and the turbine throat. In the new code with internal blade row calculating stations, it is assumed that there are no losses from the next upstream quasi-orthogonal to the throat. This would be the leading edge if no internal planes are included. In rotors of radial turbines and in turbines with a high flare, there may be a radius change between the stations. This needs to be taken into account to determine the local relative total pressure and temperature at the throat. These can be determined from the values at the upstream calculating plane on the assumption of adiabatic isentropic flow and from the condition that the rothalpy is conserved in the impeller. For choked turbine outlets the effect of supersonic deviation needs to be included, and in the throughflow code this causes the outlet flow angle in supersonic flow to be determined from the continuity equation rather than from correlations.

Choking at a compressor inlet is more complex as it can occur through three separate mechanisms, see Ref. [11]. First, if the inlet flow is subsonic, choking will occur if the Mach number reaches unity at the throat between the blades. This can occur at subsonic inlet Mach numbers with high negative incidence, or at low incidence with very thick blades with high blade blockage and a small throat area. Both cases give rise to an acceleration from a subsonic flow to a Mach number of unity at the throat, so there are few additional losses caused by this process, other than incidence effects.

Second, if the inlet flow is supersonic then the blade can also choke at the throat. If the flow chokes at the throat, this implies that first there is a detached shock from the suction surface of the blade to upstream of the adjacent blade. The supersonic inlet flow becomes subsonic at this shock and then re-accelerates to be supersonic again at the throat. The relative total pressure at the throat is thus lower than that at the inlet because of the losses across the shock, and these losses are generally modeled as if they occur in a normal shock.

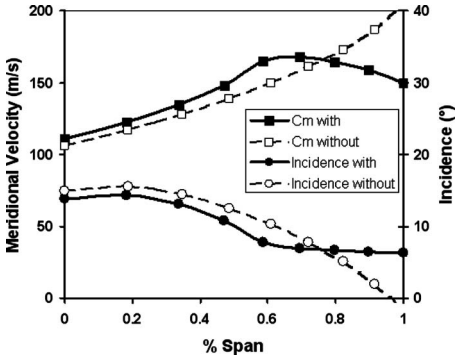

Fig. 5 The effect of the choking model on the flow and incidence distribution at inlet to a choked compressor

Third, if the inlet flow is supersonic at higher inlet Mach numbers (say $M > 1.2$) choke may occur due to unique incidence. At unique incidence, the flow in the inlet remains supersonic up to and including the throat. The flow is choked upstream of the throat by the supersonic expansion wave between the leading edge of the upper blade and the suction side. Lower incidences are not possible than the unique incidence condition, as they would imply a higher mass flow than this choking mass flow. The exact mechanism of this is explained by Freeman and Cumpsty [26] for axial compressors and has been extended to transonic radial compressors by Lohmberg et al. [27].

For choking at the throat, it is assumed that this is close to the compressor inlet and that there are no changes in relative total pressure and temperature between the inlet plane and the throat, except those which may occur in the detached shock. It is assumed that the detached shock is normal to the flow and that the shock Mach number is the same as the inlet Mach number to the blade row.

If the streamtube is choked at the throat, then this limits the maximum mass flow on this streamtube and limits the maximum meridional velocity of the flow leading to a lower limit on the incidence that is possible. Lower incidences are not possible, as they would imply a higher mass flow than the choking mass flow. In this way this mechanism for choking also produces a lower limit on the incidence as in the unique incidence condition.

At a throat, the value of the mass flow is checked during the inner iteration for mass flow in the iterative procedure. If the local value is found to be above the maximum value of a choked flow, then a limit on the meridional velocity on this streamtube is applied. The choking of an individual streamtube then automatically redistributes the mass flow across the inlet plane of a choked compressor blade row.

An example of this is given in Fig. 5. This shows the distribution of incidence and meridional velocity across the inlet plane of an industrial radial compressor. The impeller was designed for an axial inlet flow but used in a multistage machine with a radial inlet, leading to a severe gradient of the meridional velocity across the span due to the sharp inlet curvature. The calculation taking local choking into account automatically limits the mass flow in the outer choked streamtubes so that more flow enters the inner unchoked streamtubes. The same effect can be seen in the distribution of incidence in the outer streamtubes, which cannot reduce below that at choke.

Choking by unique incidence is also dealt with by applying a limit on the meridional velocity. Assuming a correlation is available for the unique incidence (i_u) or that this is known from other data, then the maximum flow angle at the leading edge on a particular streamline can be calculated from the blade angle. The swirl velocity upstream of the leading edge is known and this allows the maximum value of the meridional velocity due to unique incidence to be estimated from the blade inlet angle, as follows:

$$c_{m,\max} = c_u/\tan(\beta_1' + i_u)$$

for a stator and a similar equation with the relative swirl velocity for a rotor. If this value is less than that which would occur due to choking at the throat, then this is used to limit the meridional velocity at the leading edge plane on this streamtube.

It should be noted that choking of any particular stream-tube means that the meridional velocity of this streamtube is no longer determined by the velocity gradient equation from radial equilibrium theory, but rather by the maximum meridional velocity determined from the continuity equation. In some blade rows calculated with many internal blade calculating planes, the second and even the third calculating plane may actually be upstream of the effective throat, so an error results from the assumption that the throat is at the leading edge plane. This is taken into account in an approximate way by specifying the meridional location of the throat together with geometrical throat area as input data.

7 Iteration to Pressure Ratio

The target pressure method of Denton is used to converge the iteration to a prescribed pressure ratio. In this mode, the operating point is defined by the expansion ratio for turbines (or pressure ratio for compressors) between the inlet stagnation pressure and the static pressure at the trailing edge of the last blade row on the midspan streamline. At all other trailing edges a value for the static pressure on the midspan streamline is estimated, whereby these pressures are called the target pressures. These estimates can be approximated, as they are improved during the iteration procedure to be consistent with the mass flow through the machine and the specified overall pressure ratio.

During the iterations the normal internal mass flow iteration procedure is used at all planes which are not trailing edges, in that the meridional velocity distributions are obtained from Eq. (1) to satisfy continuity with the current value of the inlet mass flow. At trailing edge planes a different procedure is used. Here the meridional velocity on the midstreamline is adjusted not to match continuity but to achieve the target midspan static pressure. The difference between the actual pressure and the target pressure is used to correct the estimate of the meridional velocity on these planes as follows:

$$\delta c_m = -\frac{p_{\text{target}} - p}{\rho c_m}\cos^2\beta$$

This can be derived from the Euler equation, using the assumption that a small change in meridional velocity does not change the losses or the relative flow outlet angle. The corresponding mass flow at the trailing edge is then found by integration of Eq. (1). In the first instance, there is no attempt to satisfy continuity with the inlet mass flow. The program continues for a maximum number of outer iterations, at which point the target pressures will have been achieved with sufficient accuracy or fewer, if the target pressure has already been achieved.

At this point the estimates of target pressures and the inlet mass flow are revised. The estimates of target pressure are adjusted to improve agreement between the mass flow through the next downstream trailing edge and the current estimate of the inlet mass flow, using the simple correction formula

$$p_{i-1}^{N} = p_{i-1}^{N-1}\frac{\dot{m}_{\text{inlet}}^{N-1}}{\dot{m}_i^{N-1}}$$

where N is the number of the outer iteration. The change in target pressure is relaxed to ensure stability. The inlet mass flow is then updated to be that through the first trailing edge plane. The inlet mass flow is also relaxed.

In a choked compressor blade row, the losses within the bladed region are no longer a function of the mass flow, which is fixed, but become a function of the back pressure. This is rather like the situation in a choked inviscid 1D converging-diverging Laval nozzle, where the back pressure determines the location and strength of the shock, and the level of losses that occur are a function of the shock strength. At lower back pressures in a 1D Laval nozzle the shock moves backward in the diverging channel and becomes stronger with more losses at the same time. The shock losses in a choked compressor blade row are modeled in a similar way.

The equations given above are first used to identify the maximum mass flow at the throat plane. If the flow is choked and the calculation is at a specified pressure ratio, then additional losses need to be generated within the blade row so that the mass flow at outlet (where the target pressure is specified) matches the choked mass flow. Without additional losses the outlet density would be too high, and the mass flow on the blade trailing edge would be too large. The additional losses are distributed evenly across the span and uniformly downstream of the first calculating plane which is unchoked. In each iteration, the additional losses are determined from the condition needed to correct the mass flow at the trailing edge. This algorithm assumes that when the target pressure is achieved ($dp=0$), then from the Gibbs function we have

$$Tds = dh - vdp, \quad ds = dh/T = c_p(dT/T)$$

The equation for an ideal gas can be differentiated to give

$$pv = RT, \quad \frac{d\rho}{\rho} = \frac{dp}{p} - \frac{dT}{T}$$

and if $dp=0$ these equations can be combined to give

$$ds = -c_p(d\rho/\rho)$$

The error in the density is assumed to be related to the error in the mass flow at the trailing edge, so we obtain that the additional losses that are needed to match the mass flow at the trailing edge with the choked mass flow at the inlet can be estimated from the trailing edge mass flow error as

$$\Delta s \approx -c_p(\Delta\dot{m}/\dot{m})$$

The error in the mass flow at the trailing edge is thus used to update the losses within the blade row until both the mass flow, and the target pressures at the trailing edge are correct. In this process the change in the additional losses is damped in each iteration. The additional losses in this process are determined by the program and are in addition to any losses that may be specified by the user or determined by the specified correlations. Few engineers are aware of this feature of choked flow calculations, whereby the level of losses are determined directly from the pressure (or density) ratio rather than the detailed aerodynamics of the blading.

8 Equation of State

Internally the losses are defined via a change in entropy using an entropy loss coefficient, and the total enthalpy is determined by the Euler equation, so that the form of the equation of state that is most useful is

$$p = f(h,s), \quad \rho = f(h,s)$$

Many loss coefficients used in turbomachinery correlations are defined not as entropy loss coefficients but as pressure loss coefficients, so the code internally converts these to entropy losses so that the operation with the equation of state always involves the parameters h and s, and the subroutines involving the equation of state remain relatively simple.

The forms of the ideal gas equations used by the throughflow code can be derived by integration of the Gibbs equation for an ideal gas, and lead to the following equations:

$$p_2/p_1 = (h_2/h_1)^{\gamma/(\gamma-1)}e^{(s_2-s_1)/R}$$

$$\rho_2/\rho_1 = (h_2/h_1)^{1/(\gamma-1)}e^{(s_2-s_1)/R}$$

The Gibbs equation can also be integrated to find the equation for the pressure in an incompressible calculation, as follows:

$$p_2 - p_1 = \rho[(h_2 - h_1) - c_pT_1(e^{(s_2-s_1)/c_p} - 1)]$$

together with an equation for the density, which is constant.

In the case of real gases, the real gas properties are currently being incorporated via tables of values rather than as equations of state, as this procedure is only needed once for all possible gases. For reasons of consistency with other codes, the real gas data are provided to the code in the form of tables of properties in the form of

$$h = f(p,T), \quad \rho = f(p,T)$$

in a standard file format known as real gas property files (.rgp files) within the ANSYS CFX software system.

At each step in the streamline curvature iteration procedure the values of h and s are updated from the losses and the Euler equation. The throughflow code then corrects the other gas properties to find better estimates from the real gas tables. In this process the values of p^* and T^* are first taken from the previous iteration (here denoted by an asterisk) and corrected to give an improved estimate consistent with h and s.

First the value of T' consistent with the new value of h and earlier value of p^* is found from table of properties such that

$$h = f(p^*,T')$$

Then a new value of s' consistent with T' and p^* is found from

$$s' = f(p^*,T')$$

together with a new value of density (specific volume) consistent with T' and p^*

$$v' = f(p^*,T')$$

Finally, the Gibbs equation is used to find a better estimate of the pressure p' as follows:

$$Tds = dh - vdp, \quad dh = 0, \quad dp = -Tds/v$$

$$p' = p^* - (T'/v')(s' - s)$$

These steps could then be repeated to convergence, but as this process is embedded within the streamline curvature iterations, it automatically converges on the correct value when the whole solution has converged.

9 Meanline Calculation

A novel feature of the code is its ability to run as a quasi-meanline method. In this process the spanwise velocity gradient (Eq. (1)) can be multiplied by a user-specified factor less than unity. If a factor of zero is used, then the code effectively becomes a meanline code with no spanwise variation in meridional velocity. Other parameters, such as the blade speed, still vary across the span, so it is not exactly a mean-line code, but is close to this if combined with the use of correlations operating only along the mean streamline.

Clearly as a mean-line code it has a large overhead in computational effort, but this has advantages if only one code needs to be developed and maintained and ensures consistency between mean-line and through flow approximations. This feature can also be extremely useful for debugging and for analysis of difficult cases, as it allows the program to avoid divergence due to high spanwise velocity gradients during early iterations. Even very difficult cases converge readily with a reduced spanwise gradient. This ensures that the axial matching along the mean streamline of the blade rows is approximately correct, and when converged it is

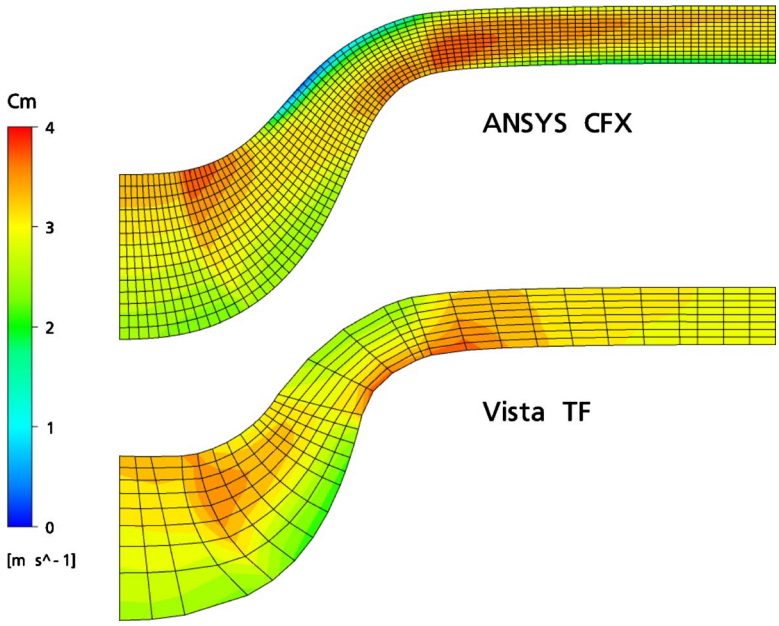

Fig. 6 Comparison of the meridional flow of a mixed flow pump compared with a 3D CFD calculation (ANSYS CFX)

possible to approach the correct solution with the correct radial distributions by slowly relaxing the value of the velocity gradient multiplication factor toward unity.

10 Validation and Verification

The code has been verified by calculation of a range of simple cases with analytical solutions, and validated by comparison with other throughflow codes, where possible.

A streamline curvature code cannot be expected to reproduce the fine details of any real flow, so measured flow distributions have not been used to validate the models of the code. In many cases predictions of the code have been compared with 3D CFD simulations, as shown in the examples already given in Figs. 2 and 4 above. Figure 6 compares the 3D CFD (ANSYS CFX) and throughflow (VISTA TF) predictions of the mean meridional velocity in a mixed flow pump with an axial diffuser operating close to its design point. In this case the impeller simulations used a slip factor correlation, and the losses are uniformly distributed. Figure 7 shows a further comparison of the mean meridional velocity distribution for a mixed flow radial turbine. In this case the outlet flow angle has been determined from the cosine rule with a correction for the underturning of the tip leakage flow, and losses are again uniformly distributed. The level of agreement in both cases is extremely good, especially taking into account a uniform distribution of losses were used, and identify clearly that the tool is sufficiently accurate for preliminary design.

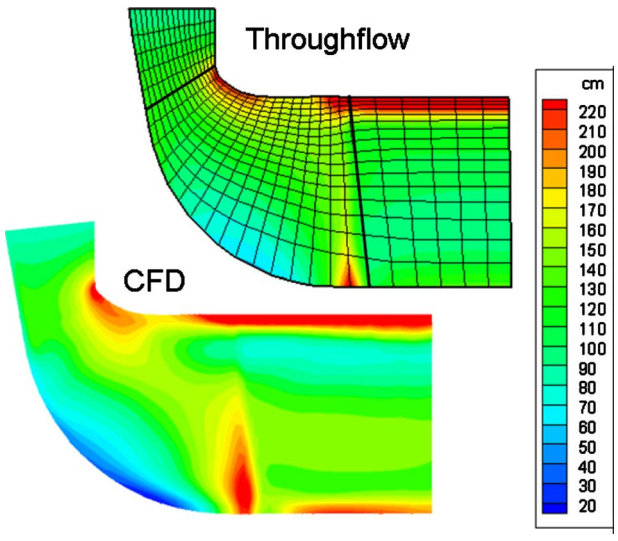

Fig. 7 Comparison of the meridional flowfield of a mixed flow turbine compared with a 3D CFD calculation (ANSYS CFX)

11 Conclusions

With suitable empirical correlations, the new throughflow code is able to closely match 3D CFD simulations for radial and mixed flow machines. Owing to its speed (seconds rather than hours), and ease of use, it is eminently suitable for preliminary design calculations. Clearly the code cannot replace more modern 3D methods in the later detailed design, but it has an important role in an integrated turbomachinery design process (see Ref. [28]) and in automated preliminary design optimization [29].

Newly developed features of the current code are as follows:

- the general methods for including losses with entropy loss coefficients and dissipation coefficients
- a new diffusion-based spanwise mixing model, which adds relatively little additional complexity to the basic method
- iteration to pressure ratio for compressors
- the models for choking of compressor blade rows taking account of the redistribution of the flow due to choking
- the ability to use the code as a quasimean-line code
- the implementation of different equations of state for liquids, ideal gases and real gases

It is currently planned that the code will be integrated as part of a future release of the ANSYS BLADEMODELER software.

Acknowledgment

Acknowledgment is given to helpful discussions with John Dunham and Peter Came of PCA Engineers Ltd. The authors would also like to thank Peter Gerkens and Richard Backhouse for support with Fortran issues, Prof. Andrew Gerber for discussions

related to real gas interpolation models, and Udo Seybold, Rob Broberg, Beat Ribi, Graham Cox, and Jason Wu for the supply of test cases. In addition the comments from the unknown reviewers of the paper have also been useful.

Nomenclature

c = absolute flow velocity
c_d = dissipation coefficient
f = mixing factor
F_d = dissipation force
h = specific enthalpy
i_u = unique incidence
i, j = indices (calculating planes and streamlines)
m = distance along meridional direction
$\dot{m}$ = mass flow rate
M = Mach number
N = number of outer iteration
o = throat width
p = static pressure
P = parameter (h_t, rc_u, or s)
q = distance along calculating plane
T = temperature
r = radius
r_c = radius of curvature
R = gas constant
s = specific entropy
S = entropy
u = blade speed
w = relative flow velocity
z = axial coordinate
Z = number of blades

Greek Symbols

β = relative flow angle
γ = blade lean angle
γ_{in} = blending function at inlet
γ_{out} = blending function at outlet
ε = diffusion coefficient
ψ = angle between streamline and plane
θ = circumferential coordinate
ρ = density

Subscripts

m = meridional component
t = total conditions
u = circumferential component

References

[1] Smith, L. H., 1966, "The Radial Equilibrium Equation of Turbomachinery," ASME J. Eng. Power, **88**, pp. 1–12.
[2] Novak, R. A., 1967, "Streamline Curvature Computing Procedures for Fluid Flow Problems," ASME J. Eng. Power, **89**, pp. 478–490.
[3] Denton, J. D., 1978, "Throughflow Calculations for Axial Flow Turbines," ASME J. Eng. Power, **100**, pp. 1978.
[4] Wu, C. H., 1952, "A General Theory of Three-Dimensional Flow in Subsonic, and Supersonic Turbomachines of Axial, Radial and Mixed-Flow Types," Trans. ASME, **74**, pp. 1363–1830.
[5] Simon, J., and Léonard, O., 2005, "A Throughflow Analysis Tool Based on the Navier-Stokes Equations," *Proceedings of the Sixth European Turbomachinery Conference*, Lille, France.
[6] Liu, B., Chen, S., and Martin, H. F., 2000, "A Primary Variable Throughflow Code and Its Application to Last Stage Reverse Flow in LP Steam Turbine," *Proceedings of the International Joint Power Generation Conference*, Miami Beach, FL, Jul. 23–26, Paper No. IJPGC2000-15010.
[7] Spurr, A., 1980, "Prediction of 3D Transonic Flow in Turbomachines Using a Combined Throughflow and Blade-to-Blade Time Marching Method," Int. J. Heat Fluid Flow, **2**(4), pp. 189–199.
[8] Marsh, H., 1968, "A Digital Computer Program for the Through-Flow Fluid Mechanics in an Arbitrary Turbomachine Using a Matrix Method," ARC R and M Report No. 3509.
[9] Casey, M. V., and Roth, P., 1984, "A Streamline Curvature Throughflow Method for Radial Turbocompressors," IMechE Conference, Paper No. C57/84.
[10] Wilkinson, D. H., 1970, "Stability, Convergence, and Accuracy Of Two-Dimensional Streamline Curvature Methods Using Quasi-Orthogonals," IMechE Convention, Glasgow, UK, Paper No. 35.
[11] Cumpsty, N. A., 2004, *Compressor Aerodynamics*, 2nd ed., Krieger Scientific, New York.
[12] Schobeiri, M., 2005, *Turbomachinery Flow Physics and Dynamic Performance*, Springer, Berlin.
[13] Horlock, J. H., 1971, "On Entropy Production in Adiabatic Flow in Turbomachines," ASME J. Basic Eng., **93**(4), pp. 587–593.
[14] Denton, J. D., 1993, "Loss Mechanisms in Turbomachines," ASME J. Turbomach., **115**, pp. 621–656.
[15] Brown, L. E., 1972, "Axial Flow Compressor and Turbine Loss Coefficients: A Comparison of Several Parameters," ASME Paper No. 72-GT-18.
[16] Casey, M. V., 2007, "Accounting for Losses and Efficiency Definitions in Turbomachinery Stages," Proc. Inst. Mech. Eng., Part A, **221**, pp. 735–743.
[17] Stanitz, J. D., and Prian V. D., 1951, "A Rapid Approximate Method for Determining Velocity Distribution on Impeller Blades of Centrifugal Compressors," Report No. NACA TN 2421.
[18] Traupel, W., 1977, *Thermische Turbomaschinen*, 3rd ed., Springer, Berlin.
[19] Smith, L. H., 2002, "Axial Compressor Aero-Design Evolution at General Electric," ASME J. Turbomach., **124**, pp. 321–330.
[20] Wilkinson, D. H., 1969, "Streamline Curvature Methods for Calculating the Flow in Turbomachines," English Electric, Whetstone, England, Report No. W/M(3F), p. 1591.
[21] Denton, J. D., and Hirsch, C., 1981, "Throughflow Calculations in Axial Turbomachines," AGARD Advisory Report No. 175.
[22] Adkins, G. G., and Smith, L. H., 1982, "Spanwise Mixing in Axial Flow Turbomachines," ASME J. Eng. Power, **104**, pp. 97–110.
[23] Gallimore, S. J., 1986, "Spanwise Mixing in Multistage Axial Flow Compressors: Part II Throughflow Calculations Including Mixing," ASME J. Turbomach., **108**, pp. 10–16.
[24] Lewis, K. I., 1994, "Spanwise Transport in Axial-Flow Turbines: Part 2–Throughflow Calculations Including Mixing," ASME J. Turbomach., **116**, pp. 187–193.
[25] Came, P. M., 1995, "Streamline Curvature Throughflow Analysis," VDI-Ber., **1185**, pp. 291–301.
[26] Freeman, C., and Cumpsty, N. A., 1989, "A Method for the Prediction of Supersonic Compressor Blade Performance," ASME Paper No. 89-GT-326.
[27] Lohmberg, A., Casey, M., and Ammann S., 2003, "Transonic Radial Compressor Inlet Design," Proc. Inst. Mech. Eng., Part A, **217**, pp. 367–374.
[28] Robinson, C. J., and Casey, M. V., 2007, "Towards a More Integrated Multidisciplinary Turbomachinery Design Process," Keynote Presentation, First International Aerospace CFD Conference, La Villette, Paris, Jun. 18–19.
[29] Casey, M. V., Gersbach, F., and Robinson, C. J., 2008, "A New Optimization Technique for Radial Compressor Impellers," ASME Paper No. GT2008-50561.